Rock and Soil Mechanics

Volume 41 | Issue 10 Article 4

3-10-2021

Hysteresis incremental model of soil-water characteristic curve based on pore expansion and contraction

CHEN Ke

CAO Wen-gui
cwglyp@hnu.edu.cn

CHEN He

Rock and Soil Mechanics 2020 41(10): 3236−3244 ISSN 1000−7598
https: //doi.org/10.16285/j.rsm.2019.7054 rocksoilmech.researchcommons.org/journal

Hysteresis incremental model of soil-water characteristic curve based on pore expansion and contraction

CHEN Ke, CAO Wen-gui, CHEN He
College of Civil Engineering, Hunan University, Changsha, Hunan 410082, China

Abstract: The void ratio of soil has an important influence on the soil-water characteristic curve (SWCC) of unsaturated soil. Experimental studies have shown that pores expand or contract under different hydraulic load paths, which results in the hysteresis of the soil-water characteristic curve (SWCC). Based on this finding, this paper assumes that the expansion and contraction of pores can cause the hysteresis of the soil-water characteristic curve (SWCC). In this study, axial translation technique is employed as an example to explain the expansion and contraction of soil pores under hydraulic loading. Then, an incremental equation for the soil-water characteristic curve that can describe the hysteresis is derived. In this equation, expansion and contraction of pores are calculated by assuming β_d to be a constant and combining the redefined equivalent pore radius with the Fredlund-Xing equation. The proposed soil-water characteristic curve model can be used to predict other scanning curves by simply using the model parameters obtained from the main drying curve and an arbitrary scanning curve. Finally, the applicability of the proposed model to different soil types is verified using five data sets obtained from tests. It is also shown that the proposed model is capable of predicting high-order scanning curves.

Keywords: unsaturated soil; soil-water characteristic curve; hysteresis effect; scanning curve; pore expansion and contraction

1 Introduction

The matrix suction−saturation curve (also known as the soil-water characteristic curve, SWCC) is of great significance for describing the mechanical properties of unsaturated soils. It is widely used in the estimation of the shear strength, volume deformation and permeability of unsaturated soils[1−3]. A large number of studies[4−6] show that SWCC is closely related to hydraulic load paths, and SWCC under different hydraulic load paths has obvious hysteresis characteristics, that is, the non-one-to-one correspondence between matrix suction and saturation during drying and wetting. Therefore, in order to reduce the engineering calculation error, the establishment of the SWCC equation that can reflect the hysteresis characteristics has important theoretical significance and practical value.

The hysteresis characteristics of SWCC have attracted wide attention from researchers[7−8]. So far, many SWCC retention equations have been proposed, which can be roughly divided into two categories. The first category is the empirical model obtained by analyzing experimental data, such as described by Li et al.[9], Scott et al.[10], Nimmo[11]. The second category is the physical model based on the hysteresis effect mechanism[12], such as contact angle hysteresis, bottleneck effect and pore expansion and contraction. The contact angle hysteresis model[13−16] suggests that changes in the surface tension of the liquid and the free energy of the system cause differences in the wet and dry contact angles, as well as the advancing and receding contact angles. The effect of this difference on water holding capacity of unsaturated porous media results in hysteresis in SWCC. The bottleneck effect model[17−20] attributes the hysteresis to the uneven distribution of pore size and irregular shape. During the wetting and drying process, the fluid movement in the irregular pores exhibit transition behavior[21−22] (called the Haines transition), resulting in hysteresis characteristics of unsaturated soil SWCC. However, the hysteresis effect caused by the mechanism of pore expansion and contraction is limited to experimental studies[23−26]. For example, Sharma[23] studied the influence of porosity changes on the water-holding behavior of unsaturated soils under the separate action of hydraulic and mechanical loads. Romero[24] studied the variation law of porosity with saturation of unsaturated soil under the coupling of mechanical and hydraulic loads and its influence on the hysteresis effect of SWCC. Simms et al.[25] studied the influence of hydraulic load

Received: 4 December 2019 Revised: 9 May 2020
This work was supported by the National Natural Science Foundation of China (51879104).
First author: CHEN Ke, male, born in 1993, Master, majors in hydraulic characteristics of unsaturated soil. E-mail: kechen0216@hnu.edu.cn
Corresponding author: CAO Wen-gui, male, born in 1963, PhD, Professor, mainly engaged in teaching and research in geotechnical engineering. E-mail: cwglyp@hnu.edu.cn

on the expansion and contraction of the pore size by analyzing the evolution law of the pore distribution function under different hydraulic loads (that is, the law of pore size changing with hydraulic load). These experimental studies show that the expansion and contraction of the pores of the soil with different hydraulic load paths will cause the hysteresis in SWCC and scanning curves.

Based on this finding, this article assumes that pore expansion and contraction can cause hysteresis in SWCC and scanning curves and establishes a mesoscopic model that can describe the expansion and contraction of soil pores under hydraulic loads based on the principle of axis translation technique. Then the equivalent radius of the pore defined by the variable cross-section capillary model is combined with the Fredlund-Xing equation to derive a SWCC and scan curve incremental model that considers pore expansion and contraction and reflects the hysteresis effect. Parameters that are necessary for using this model can be simply determined from the main drying curve and an arbitrary scan curve. That is, this model is capable of predicting other scan curves with known parameters.

2 Mesoscopic model of pore expansion and contraction

As it is widely known, the complex pore structure in soil makes its hydraulic behavior path-dependent. Studies have shown [23–26] that changes in soil porosity have a significant impact on the water-holding behavior of unsaturated soils, and different load types (mechanical loads or hydraulic loads) and their paths have different effects on the porosity of unsaturated soil. As shown in Fig. 1[26], under the action of mechanical load path $A \rightarrow B \rightarrow C$ and hydraulic load path $C \rightarrow D \rightarrow E$ (see Fig. 1(a)), the soil porosity has changed significantly. The pore deformation under mechanical load can only be partially restored, and the soil pore deformation under hydraulic load can be restored to a large extent (see Fig. 1(b)). On the other hand, the two different stress paths of hydraulic load $C \rightarrow D$ and $D \rightarrow E$ cause differences in the path of changing soil porosity. In other words, under different hydraulic paths, the change of void ratio exhibits a hysteresis effect. This is the cause of the hysteresis observed from the SWCC (see Fig.1(c)). It should be pointed out that this article only considers soils with wet expansion and dry shrinkage properties. This property is related to the type of soil and its stress state. This article does not investigate soils with wet shrinkage properties. Since the difference in void ratio with changes in hydraulic load involves the change of soil micro-pores, in order to study this physical property, it is necessary to establish a meso-analysis model that considers changes in pore size with hydraulic load.

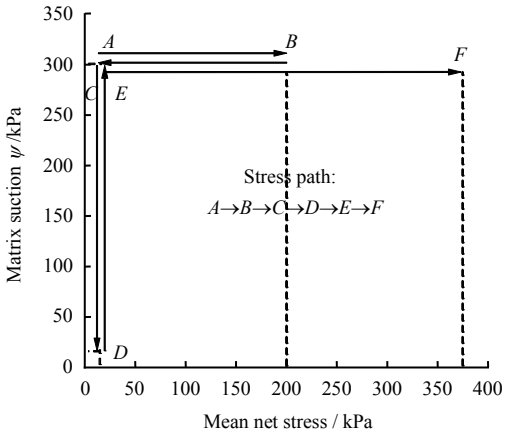

(a) Stress path

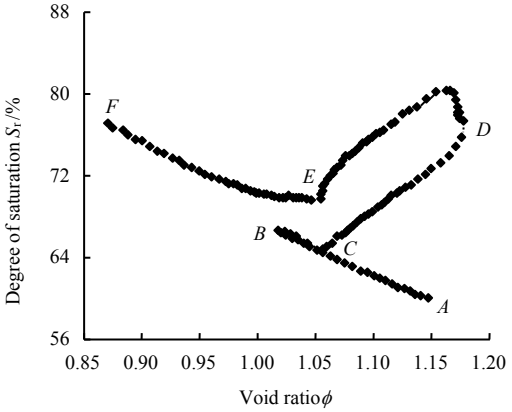

(b) Variation of void ratio with degree of saturation under different load paths

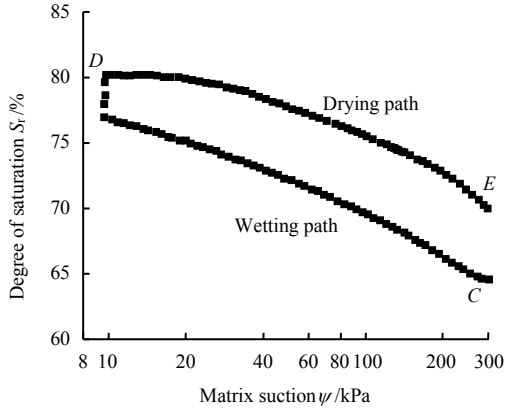

(c) Soil-water characteristic curves under different stress paths

Fig. 1 The effect of different loads and stress paths on void ratio and SWCCs[26]

This paper takes the axis translation technique as an example to explain the mesoscopic behavior of soil

pores expansion and contraction under hydraulic load. Figure 2(a) is a schematic diagram of the interface between the unsaturated soil specimen and the ceramic plate with high air entry value in the axis translation technique. As shown in Fig.2(a), the ceramic plate with high air entry value was saturated before the test, so that it only allowed water to pass through. Here we take the hydraulic unloading path (wetting process) as an example. The completely dry soil specimen is subjected to a wetting test, that is, the air pressure u_a is reduced, so that water enters the soil specimen from the porous ceramic plate. The soil specimen enters a steady state after a long enough time under a certain air pressure value u_a, water pressure u_w and a water head h_0 in the pore of the soil specimen. The process that the pressure comes to an equilibrium can be simplified as Fig. 2(b).

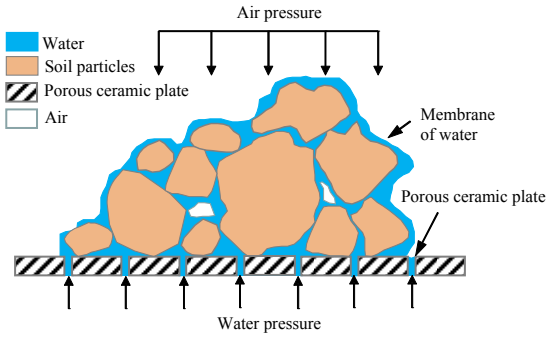

(a) Schematic diagram of the interface between the unsaturated soil specimen and the ceramic plate with high air entry value

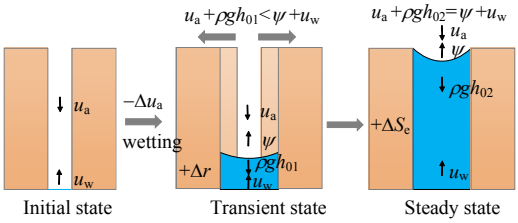

(b) Schematic diagram of pore expansion and contraction

Fig. 2 Pore expansion and contraction model under hydraulic loading

Comparing Fig.1 and Fig. 2(b), when the hydraulic load decreases ($C\rightarrow D$ in Fig.1(a)), $\psi+u_w>u_a+\rho gh_0$, the soil specimen is in the wetting process (Fig.1(c)), and pores expand. Macroscopically, the void ratio f increases ($C\rightarrow D$ in Fig.1(b)). In the same way, when the hydraulic load increases ($D\rightarrow E$ in Fig. 1(a)), $\psi+u_w<u_a+\rho gh_0$, the soil specimen is in the drying process. Pores shrink and macroscopically, the void ratio f decreases (Fig. 1(b)) in $D\rightarrow E$). When the system is in an equilibrium state in terms of pressure, $\psi+u_w=u_a+\rho gh_0$, the suction can be calculated using $\psi=u_a-u_w+\rho gh_0$. Since ρgh_0 is relatively small compared to u_a-u_w, it is negligible. Then the matrix suction can be expressed as $\psi=u_a-u_w$. Combining it with the Young-Laplace equation, we get

$$\psi=u_a-u_w=\frac{C}{r} \tag{1}$$

where $C=2\sigma\cos\theta$, σ is the surface tension of water, θ is the contact angle; ψ is the matrix suction; and r is the equivalent radius of soil pores.

It can be seen from Eq. (1) that the matrix suction of the soil is inversely proportional to the equivalent radius of soil pores. Therefore, during the dry-wet cycle of the soil, the expansion and contraction of pores will cause the soil with the same moisture content to have different matrix suctions in different processes (wetting or drying), which will lead to the hysteresis in the water holding behavior of the soil. However, the uniform capillary model in Fig.2(b) cannot describe the inhomogeneity of the pore structure in the porous medium. In order to describe the inhomogeneity of the pore structure, this paper introduces a variable cross-section capillary model as shown in Fig. 3[18]. In Fig. 3, R is the pore radius. βR is the pore throat radius, L and λL are the lengths of the pore and pore throat, respectively, where $0<\beta\leqslant 1$, $\lambda>0$. Using the geometric relationship in Fig. 3, the equivalent radius r can be calculated as

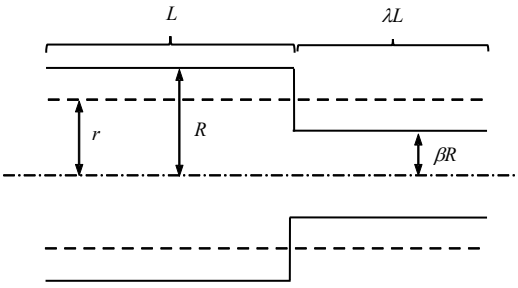

Fig. 3 Capillary model with variable cross-section

$$r=\sqrt{\frac{1+\beta^2\lambda}{1+\lambda}}R \tag{2}$$

where β and λ depict the inhomogeneity of pores. In the process of pore expansion and contraction, only the pore size changes, while the total length of the pore remains practically unchanged, so λ can be approximated as a constant.

3 Hysteresis equation for scanning curves

In general, the relationship between degree of saturation

and matrix suction is defined as unsaturated soil water retention curve or soil-water characteristic curve (SWCC). In order to describe the hysteresis characteristics of the SWCC boundary curve and the scanning curve, the main boundary (main drying or main wetting) curve is usually used as the reference curve[27−28]. The Fredlund-Xing model [29] and the VG model [30] are usually used as the boundary curve equation. In this paper, the Fredlund-Xing model is used as the main drying reference curve to study the hysteresis in water-holding behavior of unsaturated soils, namely

$$S_e = \{\ln[e + (\psi_d / a_d)^{n_d}]\}^{-m_d} \quad (3)$$

where S_e is the effective degree of saturation; ψ_d is the matrix suction on the main drying curve; a_d, n_d and m_d are the fitting parameters of the main drying curve model; and e is the natural constant.

From Eqs. (1) and (2), the relationship between matrix suction ψ and pore radius R is obtained as

$$\psi = \sqrt{\frac{(1+\lambda)C^2}{R^2(1+\beta^2\lambda)}} \quad (4)$$

Similarly, the relationship between matrix suction and pore radius R on the main drying curve can be expressed as

$$\psi_d = \sqrt{\frac{(1+\lambda)C^2}{R^2(1+\beta_d{}^2\lambda)}} \quad (5)$$

where β_d is the aperture control parameter on the main drying curve.

Combining Eqs. (4) and (5), the relationship between the suction ψ on the scanning curve and the suction ψ_d on the main drying curve can be expressed as

$$\psi = \sqrt{\frac{1+\beta_d{}^2\lambda}{1+\beta^2\lambda}}\psi_d \quad (6)$$

Substituting Eq. (6) into Eq. (3), we can obtain the scanning curve equation with the main drying curve as the reference curve, namely

$$S_e = \left\{\ln\left[e + \left(\frac{(1+\beta^2\lambda)\psi^2}{(1+\beta_d{}^2\lambda)a_d{}^2}\right)^{\frac{n_d}{2}}\right]\right\}^{-m_d} \quad (7)$$

When the aperture control parameter $\beta = \beta_d$, the scanning curve degenerates to the main drying curve. It should be emphasized that this article assumes that when the hydraulic path is stable, the soil pores expand and shrink uniformly, that is, the pore size control parameter on both the main drying curve and the main wetting curve are constant. When the direction of the hydraulic path changes, pores exhibit inhomogeneous expansion and contraction, that is, pore control parameters on the scanning curve are constantly changing with the hydraulic load.

Since the hysteresis in the water-holding behavior of unsaturated soils is a process related to hydraulic path, Eq. (7) cannot be directly applied to predict SWCC and scanning curves. For this reason, it is necessary to establish an incremental relationship among the effective degree of saturation S_e, matrix suction ψ and pore size parameters β under different hydraulic paths. If we take derivative of Eq. (7)

$$dS_e = \frac{\partial S_e}{\partial \psi}d\psi + \frac{\partial S_e}{\partial \beta}d\beta = \left(\frac{\partial S_e}{\partial \psi} + \frac{\partial S_e}{\partial \beta}\frac{d\beta}{d\psi}\right)d\psi = \frac{-m_d n_d}{\psi}[\ln(e+\xi^{\frac{n_d}{2}})]^{-m_d-1}(e\xi^{-\frac{n_d}{2}}+1)^{-1}\left(1+\frac{\lambda\beta\psi}{1+\lambda\beta^2}\frac{d\beta}{d\psi}\right)d\psi \quad (8)$$

where $\xi = (1+\beta^2\lambda)\psi^2/[a_d{}^2(1+\beta_d{}^2\lambda)]$.

It can be seen from Eq. (8) that for a given increase in suction $d\psi$, part of it is caused by the increase in degree of saturation dS_e, and the other part is caused by the increase in aperture parameters $d\beta$. From the analysis that has been mentioned in previous sections of this paper, it can be seen that on the drying scan curve, β decreases with the increase of matrix suction. On the wetting−drying curve, β increases with the decrease of matrix suction. That is, when $d\psi > 0$, $d\beta < 0$; when $d\psi < 0$, $d\beta > 0$. Therefore, $[\lambda\beta\psi/(1+\lambda\beta^2)]\cdot d\beta/d\psi \leqslant 0$ is always valid. Therefore, Eq. (8) can be rewritten as

$$\frac{dS_e}{d\psi} = \frac{-m_d n_d}{\psi}[\ln(e+\xi^{\frac{n_d}{2}})]^{-m_d-1}(e\xi^{-\frac{n_d}{2}}+1)^{-1}(1-|\omega|) \quad (9)$$

$$|\omega| = \frac{\lambda\psi\beta}{1+\lambda\beta^2}\left|\frac{d\beta}{d\psi}\right| \quad (10)$$

where $|\omega|$ is the distribution coefficient of the influence of the effective degree of saturation S_e and the pore size control parameter β on the change of matrix suction and $0 \leqslant |\omega| \leqslant 1$. If $|\omega| = 0$, it means that the increase of matrix suction is all caused by the change in the degree of saturation. If $|\omega| = 1$, it means that the increase of matrix suction is all caused by the change of pore size.

Studies have shown that [31−34], when the direction of the hydraulic load path changes, the slope of the scan curve tends to 0, $dS_e/d\psi = 0$, as shown in Fig. 4. The initial point (A or C) of the scanning curve in the figure should satisfy the boundary condition $dS_e/d\psi = 0$, that is, $|\omega| = 1$. Under this condition, the change in matrix suction is completely caused by the change in pore size. Since the

aperture control parameter on the main boundary curve is a constant, the intersection of the scanning curve and the main boundary curve, that is, the end point (*B* or *D*) of the scanning curve, should satisfy the boundary condition $\mathrm{d}\beta/\mathrm{d}\psi=0$. In addition, the scanning curve is inside the main hysteresis loop. In other words, the hysteresis loop is composed of the main drying and main wetting curves. Therefore, $\beta_\mathrm{d}\leqslant\beta\leqslant\beta_\mathrm{w}$. Based on the above boundary conditions, this paper establishes a nonlinear equation to describe the nonlinear law of the change of the distribution coefficient caused by the aperture control parameter β under different hydraulic paths, namely

$$|\omega|=\begin{cases}\left(\dfrac{\beta-\beta_\mathrm{d}}{\beta_\mathrm{w}-\beta_\mathrm{d}}\right)^{\eta} & \mathrm{d}\psi>0\\ \left(\dfrac{\beta_\mathrm{w}-\beta}{\beta_\mathrm{w}-\beta_\mathrm{d}}\right)^{\eta} & \mathrm{d}\psi<0\end{cases} \tag{11}$$

where η（$0<\eta<1$）is the nonlinear changing parameter of the pore size, which determines the distribution ratio of the pore size control parameter increment $\mathrm{d}\beta$ and the degree of saturation increment $\mathrm{d}S_\mathrm{e}$ to the matrix suction increment $\mathrm{d}\psi$. It can be seen from Eq. (11) that for the initial stage of the scanning curve, $\beta=\beta_\mathrm{d}$ ($\mathrm{d}\psi<0$) or $\beta=\beta_\mathrm{w}$ ($\mathrm{d}\psi>0$), $|\omega|=0$ satisfies the boundary conditions (point *C*, point *A*) in Fig. 4. For the final stage of the scanning curve, $\beta=\beta_\mathrm{w}$ ($\mathrm{d}\psi<0$) or $\beta=\beta_\mathrm{d}$ ($\mathrm{d}\psi>0$), $|\omega|=1$ which also satisfies the boundary conditions (point *D*, point *B*) in Fig. 4.

Substituting Eq. (7) into Eq. (9) we get

$$\frac{\mathrm{d}S_\mathrm{e}}{\mathrm{d}\psi}=\frac{-m_\mathrm{d}n_\mathrm{d}}{\psi}S_\mathrm{e}^{-m_\mathrm{d}(m_\mathrm{d}+1)}(1-\mathrm{e}^{-S_\mathrm{e}^{m_\mathrm{d}}+1})(1-|\omega|) \tag{12}$$

Combining Eqs. (11) and (12), we have

$$\frac{\mathrm{d}S_\mathrm{e}}{\mathrm{d}\psi}=\begin{cases}\dfrac{-m_\mathrm{d}n_\mathrm{d}}{\psi}S_\mathrm{e}^{-m_\mathrm{d}(m_\mathrm{d}+1)}(1-\mathrm{e}^{-S_\mathrm{e}^{m_\mathrm{d}}+1})\left\{1-\left(\dfrac{\beta-\beta_\mathrm{d}}{\beta_\mathrm{w}-\beta_\mathrm{d}}\right)^{\eta}\right\} & \mathrm{d}\psi>0\\ \dfrac{-m_\mathrm{d}n_\mathrm{d}}{\psi}S_\mathrm{e}^{-m_\mathrm{d}(m_\mathrm{d}+1)}(1-\mathrm{e}^{-S_\mathrm{e}^{m_\mathrm{d}}+1})\left\{1-\left(\dfrac{\beta_\mathrm{w}-\beta}{\beta_\mathrm{w}-\beta_\mathrm{d}}\right)^{\eta}\right\} & \mathrm{d}\psi<0\end{cases} \tag{13}$$

Equation (13) is the hysteresis increment equation of the scanning curve developed in this paper that can describe the hydraulic path. Equation (13) shows that the change of matrix suction is simultaneously affected by changes in degree of saturation and pore expansion and contraction. Since the main wetting curve can be regarded as the scanning curve with the starting point on the ending point of the main drying curve, the model in this paper can also predict the main wetting curve.

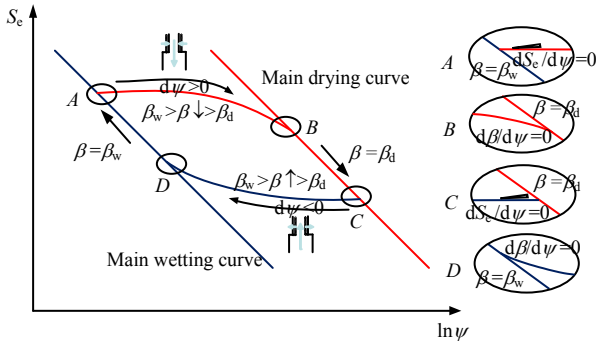

Fig. 4 A schematic diagram for boundary conditions of scanning curves

4 Determination of parameters

The scanning curve equation proposed in this paper contains six parameters: a_d, m_d, n_d, β_d, λ and η, among which a_d, m_d and n_d are the fitting parameters of the Fredlund-Xing model; and β_d and λ are the pore control parameters and η is the control parameter of change rate of pore aperture. The model parameter determination process is as follows:

(1) The parameters a_d, m_d and n_d are obtained by fitting the main drying curve data through the Fredlund-Xing model. A scanning curve is chosen arbitrarily as the parameter calibration curve and the initial point ($S_{\mathrm{e}0}$, ψ_0) of the scanning curve is determined.

(2) Set β_d ($0<\beta_\mathrm{d}<1$) and λ ($0<\lambda$) and calculate the initial value of the aperture control parameter using Eq. (6) and the initial saturation $S_{\mathrm{e}0}$.

(3) Set the parameter η ($0<\eta<1$) and calculate the initial distribution coefficient $|\omega|$ using Eq. (11) and the initial value of the aperture control parameter β_0.

(4) Set the matrix suction increment $\mathrm{d}\psi$ and use Eq. (12) to calculate the degree of saturation increment $\mathrm{d}S_\mathrm{e}$. Therefore, the next calculation point ($S_{\mathrm{e}1}$, ψ_1) can be expressed as ($S_{\mathrm{e}0}+\mathrm{d}S_\mathrm{e}$, $\psi_0+\mathrm{d}\psi$).

(5) Calculate the increment of the aperture control parameter $\mathrm{d}\beta$ using Eq. (10) and then we can obtain $\beta_1=\beta_0+\mathrm{d}\beta$.

(6) Repeat the calculation for the next point.

(7) Fit the test data and the predicted data to calibrate the parameters β_d, λ and η.

Obviously, no matter on the main boundary curve or the scanning curve, with the change of hydraulic load, the soil pores will expand and shrink unevenly. Therefore, the aperture control parameters β_d on the drying curve should also change continuously with the hydraulic load. Therefore, fitting different scan curves by the above-mentioned parameter determination method will result in different values of β_d. However, to simplify the model, it is assumed that the pore size control parameter on the

main drying curve β_d is a constant. In order to test the feasibility of this hypothesis, figures 5(a) and 5(b) show the SWCC prediction curves under constant and variable conditions, respectively and compare them with the drying-wetting cycle test data of sintered glass beads [35]. The results show that treating β_d as a constant can still better reflect the hysteresis characteristics of SWCC, so this simplification is feasible. In practical applications, if there are many scanning curve data, you can select multiple scanning curves to determine multiple values of β_d, and then take the average value to improve the accuracy of model prediction.

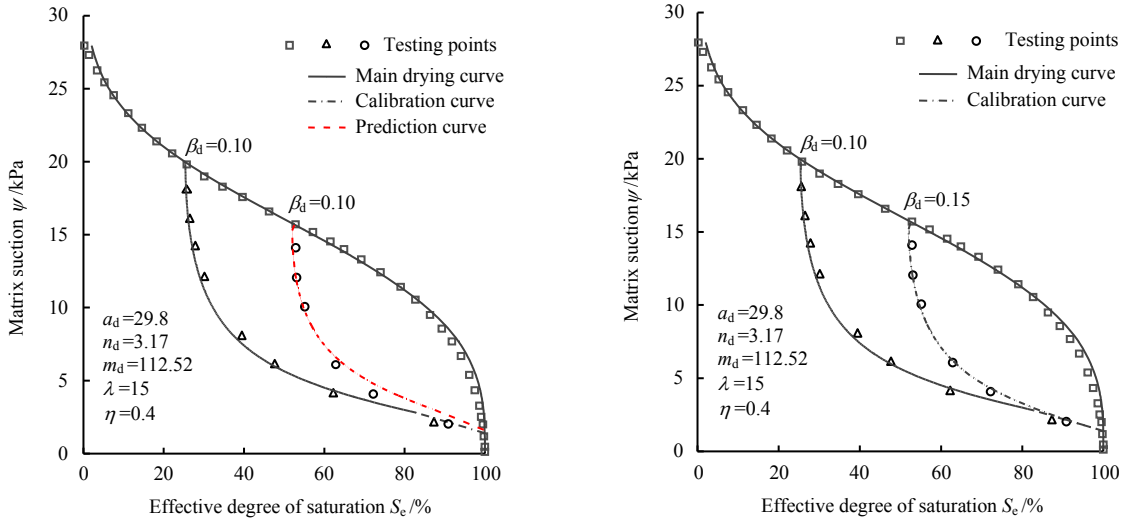

(a) β_d is a constant (b) β_d is a variable

Fig. 5 Comparison between theoretical and tested SWCCs of sintered glass beads[35]

5 Test verification

This section uses clayey silt[14], Caribou silty loam[4], silty loam[36], Houston sand[37] and the US Silica F-95 sand[38] as the testing material. 5 groups of testing data include both main drying and several scanning curves to further verifies the rationality and feasibility of the model. Model parameters obtained by the above parameter determination method are listed in Table 1.

Table 1 Parameters of SWCC and scanning curve model

Type of soil	a_d	n_d	m_d	β_d	λ	η	Source of data
Sintered glass beads	29.60	3.17	112.52	0.10	15.8	0.40	Poulovassilis[35]
Clayey silt	298.70	0.81	1.68	0.11	52.3	0.93	Azizi et al.[14]
Caribou silty loam	154.30	2.52	3.63	0.35	14.8	0.99	Topp[4]
Silty loam	1 044.50	3.90	5.31	0.51	15.3	0.61	Wei et al.[36]
Houston sand	1.66	8.67	1.01	0.46	99.8	0.98	Lins et al. [37]
the US Silica F-95 sand	12.48	6.31	49.01	0.44	16.2	0.70	Muraleetharan et al.[38]

Figure 6 shows the testing data of drying-wetting cycles of clayey silt[14]. Based on the parameter determination steps described in Section 4, the main drying curve is first fitted using the Fredlund-Xing model to obtain the parameters a_d=298.7, m_d=1.68 and n_d=0.81. β_d ($0<\beta_d<1$), η ($0<\eta<1$) and λ ($\lambda>0$) are the value range of these parameters. Arbitrarily set the initial values of β_d=0.5, η=0.3 and λ=10 within their value range to calculate the prediction curve; then compare the calculated value of the model with the test data of an arbitrarily selected scanning curve. Use the 'global search' function in MATLAB global optimization toolbox and search for the minimum root mean square error between the calculated value of the model and the experimental data, thereby determining the optimal solution of the model parameters β_d, η and λ to be β_d=0.11, η=0.93 and λ=52.3. Then the obtained model parameters can be used to predict other scanning curves. In the same way, the SWCC prediction curves of drying-wetting cycle of Caribou silty loam[4] and silty loam[36] can also be obtained by the above-mentioned parameter determination method, as shown in Figs. 7 and 8. It can be seen from Figs. 6–8 that the model prediction curve in this paper is in good agreement with the experimental data.

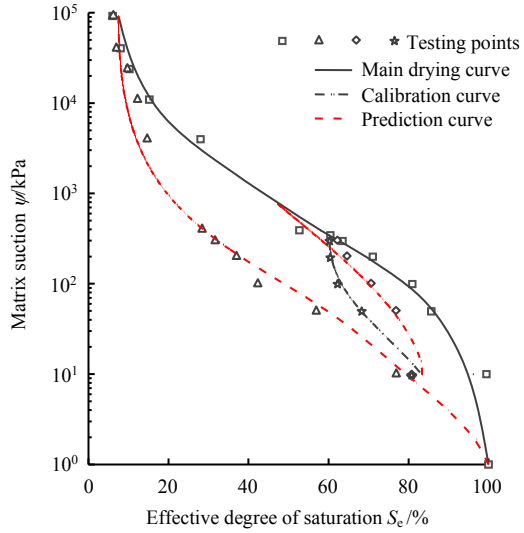

Fig. 6 Comparison between theoretical and tested SWCCs of clayey silt

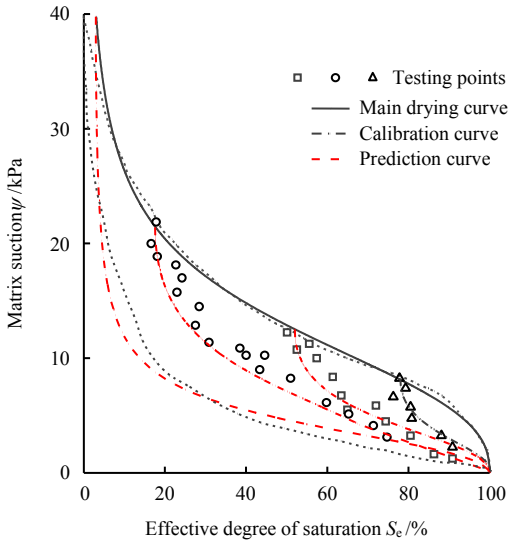

Fig. 7 Comparison between theoretical and tested SWCCs of Caribou silt loam

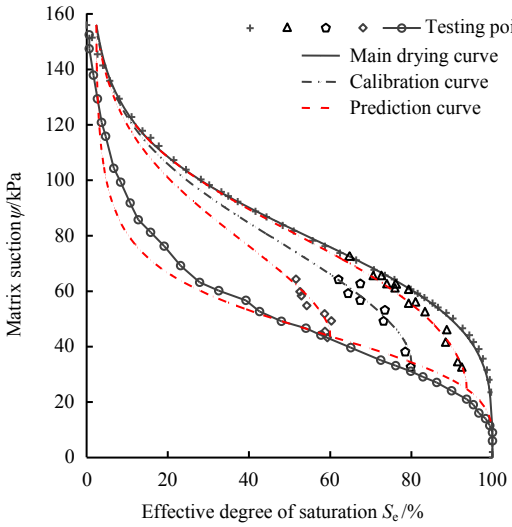

Fig. 8 Comparison between theoretical and tested SWCCs of silt loam

Figure 9 shows the curve of SWCC and pore control parameter β with hydraulic load under the hydraulic load path $A\rightarrow B\rightarrow C\rightarrow D\rightarrow E$ of Houston sand[37]. It can be observed from Fig.9(a) that the hydraulic load path $B\rightarrow C$ (wetting scanning curve) is the unloading path. β increases at this stage (see Fig. 9(b) $B\rightarrow C$). Pores expand and the influence of $\mathrm{d}\beta$ on the increment in suction $\mathrm{d}\psi$ gradually decreases. At the same time, the impact of change in degree of saturation on $\mathrm{d}\psi$ gradually increases. When the hydraulic path is changed, that is, when $B\rightarrow C$ changes to $C\rightarrow D$ (from unloading to loading), β decreases (see $C\rightarrow D$ in Fig. 9(b)). Pores shrink and the influence of $\mathrm{d}\beta$ on the increment in matrix suction $\mathrm{d}\psi$ gradually increases. At the same time, the influence of change in the degree of saturation on $\mathrm{d}\psi$ gradually increases. The increment in matrix suction $\mathrm{d}\psi$ at point D is all caused by change in degree of saturation.

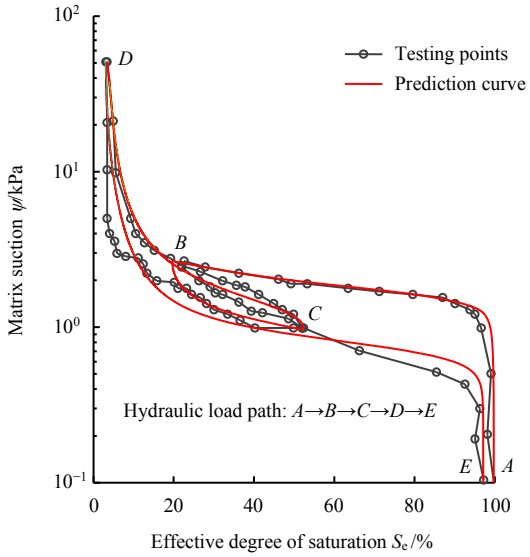

(a) Comparison of SWCC test data and prediction curve for Houston sand

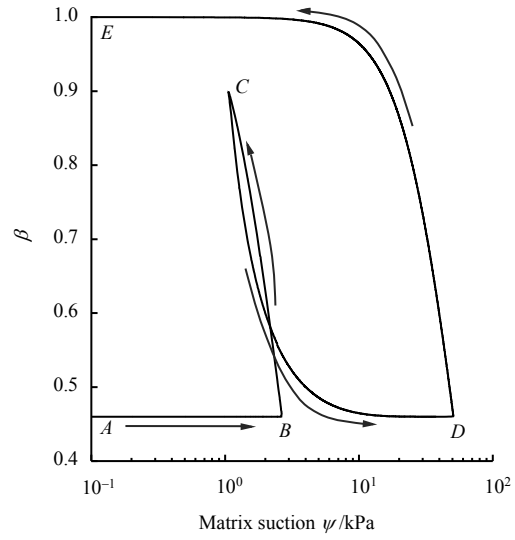

(b) The relationship curve between parameter β and matrix suction

Fig. 9 Comparison between theoretical and tested SWCCs of Houston sand and the relationship between β and suction

The SWCC model proposed in this paper can predict not only the initial scanning curve with the boundary curve as the starting point, but also predict the higher order scanning curve. Figure 10 shows the test data of drying-wetting cycle of the US Silica F-95 sand[38] and the SWCC multi-order scanning curve predicted using the model in this paper. As shown in Fig.10, the initial point *A* of the first-order wetting scanning curve is on the main drying curve. As the hydraulic load decreases (unloading), it gradually approaches the main wetting curve to point *B*. Then the hydraulic load path changes from unloading (*A*→*B*) to loading (*B*→*C*). With the continuous increase of suction, the first-order drying scanning curve completes a drying-wetting cycle from point *B* to point *C*, then it starts from point *C* and passes through the hydraulic load path *C*→*D*→*E*. Then a second-order wetting and drying scanning curve is generated. If you continue to change the direction of hydraulic load, the model in this paper can be used to predict higher order scanning curves.

The above examples suggests that the incremental model based on pore expansion and contraction proposed in this paper can better describe the hysteresis characteristics of water-holding behavior in unsaturated soils.

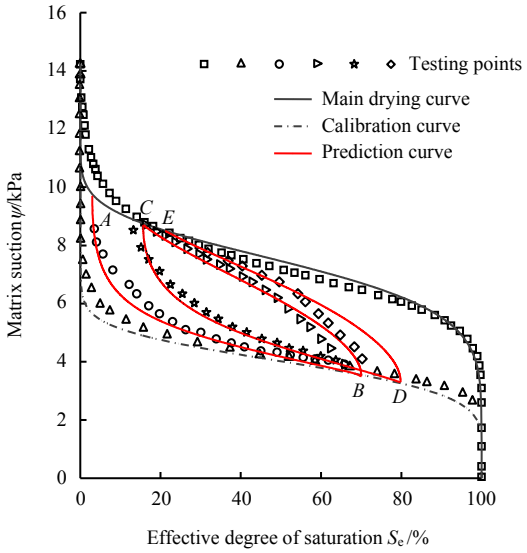

Fig. 10 Comparison between theoretical and tested SWCCs of the US Silica F-95 sand

6 Conclusion

Starting from the analysis of the SWCC and scanning curve hysteresis physical mechanism, it is assumed that changes in the degree of saturation and pore expansion and contraction of unsaturated soils can affect the change of the matrix suction, and thus the water-holding characteristics of unsaturated soils are discussed. The main conclusions are as follows:

(1) According to the existing experimental conclusions, this paper suggests that the pore expansion and contraction is the cause of the hysteresis of SWCC and scanning curves. On this basis, the axial translation technique is taken as an example to explain the mesoscopic behavior of the expansion and contraction of soil pores under hydraulic load.

(2) By combining the equivalent radius of the pore defined by the variable cross-section capillary model with the Fredlund-Xing equation, a SWCC and scanning curve incremental model that considers pore expansion and contraction and reflect the hysteresis effect is derived. By taking aperture control parameters as constants, the model is simplified. The model can be used by simply determining the parameters through the main drying curve and arbitrary scanning curves to predict other scanning curves.

(3) Five sets of test data of different soil types are used to verify the model in this paper. Results show that the model can better describe the hysteresis characteristics of SWCC and scanning curves. The model is also capable of predicting high-order scanning curves.

References

[1] ALONSO E E, PEREIRA J M, VAUNAT J, et al. A microstructurally-based effective stress for unsaturated soils[J]. Géotechnique, 2010, 60(12): 913–925.

[2] ZHOU A, SHENG D. Yield stress, volume change, and shear strength behaviour of unsaturated soils: validation of the SFG model[J]. Canadian Geotechnical Journal, 2009, 46(9): 1034–1045.

[3] ASSOULINE S. A model for soil relative hydraulic conductivity based on the water retention characteristic curve[J]. Water Resources Research, 2001, 37(2): 265–271.

[4] TOPP G C. Soil-water hysteresis: the domain theory extended to pore interaction conditions[J]. Soil Science Society of America Journal, 1971, 35(2): 219–225.

[5] CAI Guo-qing, LIU Yi, XU Run-ze, et al. Experimental investigation for soil-water characteristic curve of red clay in full suction range[J]. Chinese Journal of Geotechnical Engineering, 2019, 41(Suppl. 2): 13–16.

[6] PARKER J C, LENHARD R J. A model for hysteretic constitutive relations governing multiphase flow: 1. saturation-pressure relations[J]. Water Resources Research, 1987, 23(12): 2187–2196.

[7] LIU Yan, ZHAO Cheng-gang. Hysteresis model for soil-water characteristic curves[J]. Chinese Journal of Geotechnical Engineering, 2008, 30(3): 399–405.

[8] HE Wei, ZHAO Ming-hua, CHEN Yong-gui, et al. Theoretical study of microscopical mechanisms and computational method of hysteresis in SWCCs[J]. Rock

and Soil Mechanics, 2010, 31(4): 1078−1083.

[9] LI Huan, WEI Chang-fu, CHEN Hui, et al. A simplified capillary hysteresis model of porous media[J]. Rock and Soil Mechanics, 2011, 32(9): 2635−2639.

[10] SCOTT P S, FARQUHAR G J, KOUWEN N. Hysteretic effects on net infiltration[J]. Advances in Infiltration, 1983, 11(83): 163−170.

[11] NIMMO J R. Semi-empirical model of soil water hysteresis[J]. Soil Science Society of America Journal, 1992, 56(4): 936.

[12] NING LU, WILLIAM J LIKOS. Unsaturated soil mechanics[M]. Translated by WEI Chang-fu, et al. Beijing: Higher Education Press, 2012.

[13] ZHOU A N. A contact angle-dependent hysteresis model for soil-water retention behaviour[J]. Computers and Geotechnics, 2013, 49: 36−42.

[14] AZIZI A, JOMMI C, MUSSO G. A water retention model accounting for the hysteresis induced by hydraulic and mechanical wetting-drying cycles[J]. Computers and Geotechnics, 2017, 87: 86−98.

[15] CZACHOR H. Modelling the effect of pore structure and wetting angles on capillary rise in soils having different wettabilities[J]. Journal of Hydrology, 2006, 328(3-4): 604−613.

[16] PAYATAKES A C, NG K M, FLUMERFELT R W. Oil ganglion dynamics during immiscible displacement: model formulation[J]. AIChE Journal, 1980, 26(3): 430−443.

[17] YANG Ming-hui, CHEN He, CHEN Ke. Study of the hysteresis effect model of SWCC boundary curves based on fractal theory[J]. Rock and Soil Mechanics, 2019, 40(10): 3805−3812.

[18] MUALEM Y. Hysteretical models for prediction of the hydraulic conductivity of unsaturated porous media[J]. Water Resources Research, 1976, 12(6): 1248−1254.

[19] GUARRACINO L, ROTTING T, CARRERA J. A fractal model to describe the evolution of multiphase flow properties during mineral dissolution[J]. Advances in Water Resources, 2014, 67: 78−86.

[20] SOLDI M, GUARRACINO L, JOUGNOT D. A simple hysteretic constitutive model for unsaturated flow[J]. Transport in Porous Media, 2017, 120(2): 271−285.

[21] HAINES W B. Studies in the physical properties of soil. V. The hysteresis effect in capillary properties, and the modes of moisture distribution associated therewith[J]. The Journal of Agricultural Science, 1930, 20(1): 97−116.

[22] RICHARDS L A. Capillary conduction of liquids through porous mediums[J]. Physics, 1931, 1(5): 318−333.

[23] SHARMA R S. Mechanical behaviour of unsaturated highly expansive clays[D]. Oxford, UK: University of Oxford, 1998.

[24] ROMERO E. Characterisation and thermo-hydro-mechanical behaviour of unsaturated Boom clay: an experimental study[D]. Barcelona: Polytechnic University of Catalonia, 1999.

[25] SIMMS P H, YANFUL E K. Measurement and estimation of pore shrinkage and pore distribution in a clayey till during soil-water characteristic curve tests[J]. Canadian Geotechnical Journal, 2001, 38(4): 741−754.

[26] HU R, CHEN Y F, LIU H H, et al. A water retention curve and unsaturated hydraulic conductivity model for deformable soils: consideration of the change in pore-size distribution[J]. Géotechnique, 2013, 63(16): 1389−1405.

[27] PARLANGE J Y. Capillary hysteresis and the relationship between drying and wetting curves[J]. Water Resources Research, 1976, 12(2): 224−228.

[28] MUALEM Y. Extension of the similarity hypothesis used for modeling the soil water characteristics[J]. Water Resources Research, 1977, 13(4): 773−780.

[29] FREDLUND D G, XING A. Equations for the soil-water characteristic curve[J]. Canadian Geotechnical Journal, 1994, 31(4): 521−532.

[30] VAN GENUCHTEN M T. A closed-form equation for predicting the hydraulic conductivity of unsaturated soils[J]. Soil science society of America Journal, 1980, 44(5): 892−898.

[31] PHILIP J R. Similarity hypothesis for capillary hysteresis in porous materials[J]. Journal of Geophysical Research, 1964, 69(8): 1553−1562.

[32] POULOVASSILIS A. Hysteresis of pore water in granular porous bodies[J]. Soil Science, 1970, 109(1): 5−12.

[33] MUALEM Y. Modified approach to capillary hysteresis based on a similarity hypothesis[J]. Water Resources Research, 1973, 9(5): 1324−1331.

[34] POULOVASSILIS A, KARGAS G. A note on calculating hysteretic behavior[J]. Soil Science Society of America Journal, 2000, 64(6): 1947−1950.

[35] POULOVASSILIS A. The effect of the entrapped air on the hysteresis curves of a porous body and on its hydraulic conductivity[J]. Soil Science, 1970, 109(3): 154−162.

[36] WEI C, DEWOOLKAR M M. Formulation of capillary hysteresis with internal state variables[J]. Water Resources Research, 2006, 42(7). DOI: 10.1029/2005WR004594.

[37] LINS Y, ZOU Y, SCHANZ T. Physical modeling of SWCC for granular materials[M]//Theoretical and Numerical Unsaturated Soil Mechanics. Berlin, Heidelberg: Springer, 2007.

[38] MURALEETHARAN K K, LIU C, WEI C, et al. An elastoplatic framework for coupling hydraulic and mechanical behavior of unsaturated soils[J]. International Journal of Plasticity, 2009, 25(3): 473−490.